

Three-dimensional ferroelectric domain visualization by Čerenkov-type second harmonic generation

Yan Sheng^{1,2}, Andreas Best¹, Hans-Jürgen Butt¹, Wieslaw Krolkowski², Ady Arie³ and Kaloian Koynov¹

¹Max-Planck Institute for Polymer Research, Mainz 55128, Germany

²Laser Physics Center, Australian National University, Canberra ACT 0200, Australia

³School of Electrical Engineering, Tel-Aviv University, Tel Aviv 69978, Israel

koynov@mpip-mainz.mpg.de

Abstract: We show that focusing a laser light onto the boundary between antiparallel ferroelectric domains leads to the non-collinear generation of two second harmonic (SH) beams. The beams are emitted in a plane normal to the domain boundaries at the angles that satisfy the Čerenkov-type phase matching condition. Moreover, these beams disappear when the laser light is focused on a homogenous part of a single domain. We utilize this effect for 3-dimensional visualization of fine details of the ferroelectric domain pattern with a submicron accuracy.

© 2010 Optical Society of America

OCIS codes: (190.0190) Nonlinear optics; (190.2620) Harmonic generation and mixing; (160.2260) Ferroelectrics; (180.6900) Three-dimensional microscopy

References and links

1. M. M. Fejer, G. A. Magel, D. H. Jundt, and R. L. Byer, "Quasi-phase-matched second harmonic generation: tuning and tolerances," *IEEE J. Quantum Electron.* **28**, 2631–2654 (1992).
2. S. Zhu, Y. Y. Zhu, and N. B. Ming, "Quasi-phase-matched third-harmonic generation in a quasi-periodic optical superlattice," *Science* **278**, 843–846 (1997).
3. V. Berger, "Nonlinear Photonic Crystals," *Phys. Rev. Lett.* **81**, 4136–4139 (1998).
4. N. G. R. Broderick, G. W. Ross, H. L. Offerhaus, D. J. Richardson, and D. C. Hanna, "Hexagonally poled lithium niobate: a two-dimensional nonlinear photonic crystal," *Phys. Rev. Lett.* **84**, 4345–4348 (2000).
5. T. Ellenbogen, N. Voloch-Bloch, A. Ganany-Padowicz, and A. Arie, "Nonlinear generation and manipulation of Airy beams," *Nat. Photonics* **3**, 395–398 (2009).
6. P. Xu, S. H. Ji, S. N. Zhu, X. Q. Yu, J. Sun, H. T. Wang, J. L. He, Y. Y. Zhu, and N. B. Ming, "Conical second harmonic generation in a two-dimensional $\chi^{(2)}$ photonic crystal: a hexagonally poled LiTaO₃ crystal," *Phys. Rev. Lett.* **93**, 133904 (2004).
7. S. M. Saltiel, Y. Sheng, N. Voloch-Bloch, D. N. Neshev, W. Krolkowski, A. Arie, K. Koynov, and Y. S. Kivshar, "Čerenkov-type second-harmonic generation in two-dimensional nonlinear photonic structures," *IEEE J. Quantum Electron.* **45**, 1465–1472 (2009).
8. A. R. Tunyagi, M. Ulex, and K. Betzler, "Noncollinear optical frequency doubling in strontium barium niobate," *Phys. Rev. Lett.* **90**, 243901 (2003).
9. Y. Zhang, F. M. Wang, K. Geren, S. N. Zhu, and M. Xiao, "Second-harmonic imaging from a modulated domain structure," *Opt. Lett.* **35**, 178–180 (2010).
10. A. Fragemann, V. Pasiskevicius, and F. Laurell, "Second-order nonlinearities in the domain walls of periodically poled KTiOPO₄," *Appl. Phys. Lett.* **85**, 375–377 (2004).
11. S. Matsumoto, E. J. Lim, H. M. Hertz, and M. M. Fejer, "Quasiphase-matched second harmonic generation of blue light in electrically periodically-poled lithium tantalate waveguides," *Electron. Lett.* **27**, 2040–2042 (1991).
12. J. A. Hooton and W. J. Merz, "Etch patterns and ferroelectric domains in BaTiO₃ single crystal," *Physical Review* **98**, 409–413 (1955).

13. S. N. Zhu and W. W. Cao, "Direct observation of ferroelectric domains in LiTaO₃ using environmental scanning electron microscopy," *Phys. Rev. Lett.* **79**, 2558–2561 (1997).
14. T. Jungk, A. Hoffmann, and E. Soergel, "Contrast mechanisms for the detection of ferroelectric domains with scanning force microscopy," *New J. Phys.* **11**, 033092 (2009).
15. E. Soergel, "Visualization of ferroelectric domains in bulk single crystals," *Appl. Phys.* **81**, 729–752 (2005).
16. V. Y. Shur, E. L. Rumyantsev, R. G. Batchko, G. D. Miller, M. M. Fejer, and R. L. Byer, "Domain kinetics in the formation of a periodic domain structure in lithium niobate," *Phys. Solid State* **41**, 1681–1687 (1999).
17. G. Rosenman, K. Garb, A. Skliar, M. Oron, D. Eger, and M. Katz, "Domain broadening in quasi-phase-matched nonlinear optical devices," *Appl. Phys. Lett.* **73**, 865–867 (1998).
18. Y. Sheng, T. Wang, B. Q. Ma, E. Qu, B. Cheng, and D. Zhang, "Anisotropy of domain broadening in periodically poled lithium niobate crystal," *Appl. Phys. Lett.* **88**, 041121 (2006).
19. P. G. Ni, B. Q. Ma, X. H. Wang, B. Cheng, and D. Zhang, "Second-harmonic generation in two-dimensional periodically poled lithium niobate using second-order quasiphase matching," *Appl. Phys. Lett.* **82**, 4230–4232 (2003).
20. S. I. Bozhevolnyi, J. M. Hvam, K. Pedersen, F. Laurell, H. Karlsson, T. Skettrup, and M. Belmonte, "Second-harmonic imaging of ferroelectric domain walls," *Appl. Phys. Lett.* **73**, 1814–1816 (1998).
21. V. Grubsky, S. MacCormack, and J. Feinberg, "All-optical three-dimensional mapping of 180° domains hidden in a BaTiO₃ crystal," *Opt. Lett.* **21**, 6–8 (1996).
22. J. Harris, G. Norris, and G. McConnell, "Characterization of periodically poled materials using nonlinear microscopy," *Opt. Express* **16**, 5667–5672 (2008).
23. M. Flörsheimer, R. Paschotta, U. Kubitschek, C. Brillert, D. Hofmann, L. Heuer, G. Schreiber, C. Verbeek, W. Sohler and H. Fuchs, "Second-harmonic imaging of ferroelectric domains in LiNbO₃ with micron resolution in lateral and axial directions," *Appl. Phys. B-Lasers Opt.* **67** 593–599 (1998).
24. A. Rosenfeldt and M. Flörsheimer, "Nondestructive remote imaging of ferroelectric domain distributions with high three-dimensional resolution," *Appl. Phys. B-Lasers Opt.* **73**, 523–529 (2001).
25. Y. Uesu, H. Yokota, S. Kawado, S. Kawado, J. Kaneshiro, S. Kurimura, and N. Kato, "Three-dimensional observation of periodically poled domains in a LiTaO₃ quasiphase matching crystal by second-harmonic generation microscope," *Appl. Phys. Lett.* **91**, 182904 (2007).
26. Y. Sheng, J. Dou, B. Cheng and D. Zhang, "Effective generation of red-green-blue laser in a two-dimensional decagonal photonic superlattice," *Appl. Phys. B-Lasers Opt.* **87**, 603–606 (2007).
27. Y. Sheng, K. Koynov, and D. Zhang, "Collinear second harmonic generation of 20 wavelengths in a single two-dimensional decagonal nonlinear photonic quasi-crystal," *Opt. Commun.* **282**, 3602–3606 (2009).
28. G. J. Edwards and M. Lawrence, "A temperature-dependent dispersion equation for congruently grown lithium niobate," *Opt. Quantum Electron.* **16**, 373–375 (1984).
29. X. Deng, H. Ren, Y. Zheng, K. Liu, and X. Chen, "Significantly enhanced second order nonlinearity in domain walls of ferroelectrics," arXiv:1005.2925v1 [physics.optics] (2010).
30. K. Hayata, K. Yanagawa, and M. Koshiba, "Enhancement of the guided-wave second-harmonic generation in the form of Cerenkov radiation," *Appl. Phys. Lett.* **56**, 206–208 (1990).
31. Y. Sheng, S. M. Saltiel, and K. Koynov, "Cascaded third-harmonic generation in a single short-range-ordered nonlinear photonic crystal," *Opt. Lett.* **34**, 656–658 (2009).
32. Y. Sheng, J. Dou, B. Ma, B. Cheng, and D. Zhang, "Broadband efficient second harmonic generation in media with a short-range order," *Appl. Phys. Lett.* **91**, 011101 (2007).
33. Y. Sheng, J. Dou, B. Ma, J. Li, D. Ma, B. Cheng, and D. Zhang, "Temperature and angle tuning of second harmonic generation in media with a short-range order," *Appl. Phys. Lett.* **91**, 101109 (2007).
34. A. Bahabad, A. Ganany-Padowicz, and A. Arie, "Engineering two-dimensional nonlinear photonic quasi-crystal," *Opt. Lett.* **33**, 1386–1388 (2008).
35. I. Juwiler and A. Arie, "Efficient frequency doubling by a phase-compensated crystal in a semimonolithic cavity," *Appl. Optics* **42**, 7163–7169 (2003).
36. R. Fischer, S. M. Saltiel, D. N. Neshev, W. Krolikowski, and Y. S. Kivshar, "Broadband femtosecond frequency doubling in random media," *Appl. Phys. Lett.* **89**, 191105 (2006).
37. W. Wang, K. Kalinowski, Y. Kong, C. Cojocaru, J. Trull, R. Vilaseca, M. Scalora, W. Krolikowski, and Y. S. Kivshar, "Third-harmonic generation via broadband cascading in disordered quadratic nonlinear media," *Opt. Express* **17**, 20117 (2009).

1. Introduction

Nonlinear photonic structures (NPS) are a new class of engineered materials that have constant refractive index, but spatially modulated 2^{nd} order nonlinear susceptibility. Their development has revolutionized the field of nonlinear optics because they not only offer a new versatile way to realize efficient nonlinear optical interactions [1, 2, 3, 4], but even more importantly allow

the exploration of novel classes of light-matter interactions [5, 6]. Among the most interesting interaction schemes is, the so called, Čerenkov-type second harmonic generation (SHG) named so because of the close analogy to the famous Čerenkov effect that describes the emission of conical radiation caused by charged particle traveling faster than the speed of the light in the medium. It has been shown recently that the intensity of Čerenkov-type SHG is greatly enhanced in NPS [7, 8, 9]. The exact nature of this effect is still unclear, being attributed either to the existing of broad spectra of reciprocal vectors in NPS that contribute to the Čerenkov-type phase matching [7, 8] or to the enhancement of the 2nd order susceptibility at the inverted domains boundaries due to strong local electric fields [10].

Nowadays a variety of nonlinear photonic structures with either one- or two- dimensional periodicity or quasi periodicity are almost routinely fabricated, by e.g., electrical field-induced domain inversion in ferroelectric crystals [11]. The induced domain structures have been analyzed by selective etching [12], scanning electron microscopy [13], atomic force microscopy [14], etc. Unfortunately, these methods only provide information on the surface structure while the internal structure of NPS, which can be diverse and complex, remains inaccessible for the non-destructive observations [15]. For instance, it is known that with depth, the inverted domains undergo sidewise expansion [16], acquire preferred shapes [17, 18], and occasionally merge into a bigger domains [19]. The details about when, where and how these processes occur are largely unexplored as this requires accurate three-dimensional (3D) visualization of the inverted domains. So far, only few techniques have been used for 3D observations [20, 21, 22, 23, 24, 25], and their application was determined by the type of the media [21, 22], the thickness of the sample [21], and the presence of the reference plate [25]. Moreover, as all the existing studies were limited to 1D NPS, even less is known about internal domain structure in NPS with 2D periodicity, thus preventing further optimization of the fabrication process, designing more complex structures for advanced applications and finally understanding the origin of defect formation.

In this paper we present a new simple method for high-resolution 3D imaging of the inverted domains hidden inside NPS. It is based on the fact that tight focusing of a light beam on a single boundary between two anti-parallel ferroelectric domains leads to two second harmonic signals being emitted via the Čerenkov-type SHG in a plane normal to the domain boundary. This enables for a direct, three dimensional non-destructive imaging of the inverted domain pattern in NPS with a sub-micrometer resolution. We apply this method to study the evolution of the inverted domain structures from the surface into the material depth in several structures fabricated in different ferroelectric materials.

2. Experimental setup

A schematic representation of our experimental setup is depicted in Fig. 1(a). As excitation source we used a titanium-sapphire laser (Mai Tai, Spectra Physics) tunable in the range 780 to 920 nm and delivering ~ 100 fs pulses at 80 MHz repetition rate and up to 12 nJ pulse energy. The fundamental beam from this laser is coupled into the commercial laser scanning confocal microscope (LSM 510 + Axiovert 200, Zeiss) and tightly focused by an objective lens (Plan Apochromat 100 \times 1.46 NA) to produce a near diffraction-limited focal spot with diameter of $\sim 0.7 \mu\text{m}$ and Rayleigh length less than $2.0 \mu\text{m}$. The position of the focus can be scanned in three dimensions with the resolution better than 100 nm: in the X-Y plane by a pair of galvanometric mirrors and in the Z direction by translation of the objective lens that is mounted on a motorized stage. The second harmonic signal generated in the NPS is collected by a condenser lens and its intensity measured, by a photomultiplier, as a function of the focus position i.e. using the standard transmission mode of the microscope. A BG39 filter blocks the transmitted fundamental beam. Alternatively a color CCD camera (USB UI-2240SE, IDS) was used to directly observe the Čerenkov SH signal for a fixed position of the laser focus.

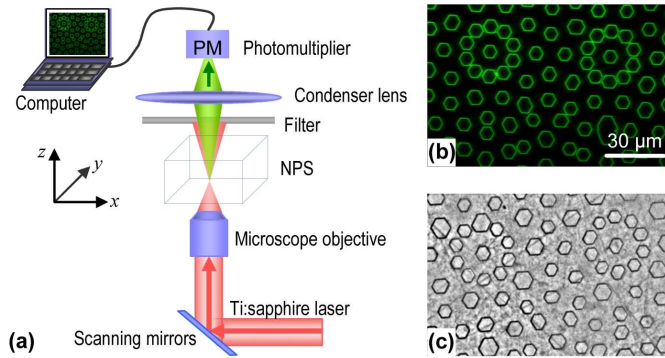


Fig. 1. (a) Schematic of the experimental setup; (b-c) Images of the inverted domain pattern of a 2D quasi-periodic NPS obtained via (b) Čerenkov SHG inside the NPS and (c) optical microscopy after selective etching of the NPS surface.

3. Results and discussion

Figure 1(b) shows a typical X-Y scan (scanning speed 1 frame/sec) of the SHG intensity from a 2D quasi-periodic NPS formed in congruent LiNbO_3 crystal [26, 27] with the focal plane located at a depth of $10 \mu\text{m}$ above the polished lower surface of the sample. Bright SH intensity patterns in a form of hexagons can be clearly seen. These hexagons represent boundaries of the inverted domains as evident from the comparison with the conventional optical microscopy image [Fig. 1(c)] obtained from the surface of similar nonlinear structure after selective chemical etching.

Figure 1(b) shows that the generated SH signal is strongly enhanced when the beam focal spot is positioned on a boundary between the inverted and non-inverted parts of the NPS. Various speculations were made previously about the origin of this effect [23]. Here we show for the first time that the second harmonic light is generated in Čerenkov-type process. To this end we modified our experimental setup, replacing the condenser lens and the photo-multiplier with a diffusive screen and a color CCD camera.

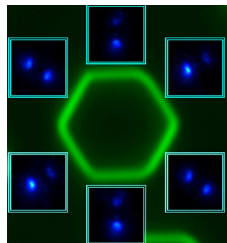


Fig. 2. SHG patterns (blue spots) imaged with a CCD camera when the fundamental beam was focused on the corresponding domain boundary of the LiNbO_3 NPS. Second harmonic spots are located symmetrically with respect to the domain wall and direction of the fundamental beam (not shown) which is perpendicular to the plane of this figure.

Figure 2 depicts the second harmonic patterns (in blue) observed on the screen above the LiNbO_3 structure when the diffraction limited focal spot of the fundamental beam ($\lambda_1 = 910 \text{ nm}$) is positioned subsequently on each of the six sides of a hexagon unit cell (shown in green). Here the fundamental beam (not shown) propagates perpendicularly to the plane of the figure. In all cases we observed two second harmonic beams emitted non-collinearly with respect to

the fundamental beam. Our earlier works showed that the Čerenkov second harmonic signal is emitted mainly in the directions corresponding to the availability of reciprocal vectors originating from the modulation of the nonlinearity [7]. Since the domain wall for a tightly focused fundamental beam is a quasi-one-dimensional object, the corresponding reciprocal vectors lie in the plane normal to the domain boundary. As a result, the strongest Čerenkov emission will take place in the same plane and hence will be visible behind the crystal as two localized spots located symmetrically with respect to the domain wall (and the direction of the fundamental beam).

The measured external angle between the second harmonic and fundamental beams was 52.4° in good agreement with the theoretical value for the Čerenkov angle of 51.0° at $\lambda_1=910$ nm [28], derived on the basis of longitudinal phase matching condition $\cos\theta = 2k_1/k_2$. Here, k_1 and k_2 are the wave vectors of the fundamental and the SH beams, respectively. These harmonic beams disappear when the focus of the fundamental beam moves away from the boundary into a homogeneous region of the domains. Furthermore, Fig. 2 shows that the directions of the generated Čerenkov SH beams lie in a plane normal to the domain boundaries. It is worth noting that similar domain wall-enhanced emission of Čerenkov second harmonic has been recently reported in [29].

A number of effects may contribute to the enhancement of Čerenkov SHG in the domain wall regions. For example, it has been suggested that the quadratic nonlinearity $\chi^{(2)}$ of ferroelectric crystals may be enhanced by the presence of a strong DC electric field created by the strain at the walls [10]. Another possible reason could be the constructive interference of the second harmonic waves generated by different parts of the fundamental beam that covers simultaneously regions belonging to two anti-parallel ferroelectric domains [8, 30]. Regardless of its exact physical origin, the strong enhancement of Čerenkov SHG emission in the area of the domain wall, is a clear experimental fact and can be employed for a direct 3D visualization of the inverted domain pattern hidden inside the NPS. In order to explore universality of this Čerenkov SHG microscopy concept, we applied it to examine the inverted domains in NPS made of different ferroelectric crystals, as shown in Fig. 3. In all cases this technique performs superbly, producing high contrast images. Furthermore, the method offers an exceptional spatial resolution, which is below the diffraction limit for the excitation laser wavelength of 820 nm. As shown in Fig. 3(e) even domain boundaries separated by less than 250 nm can be easily resolved.

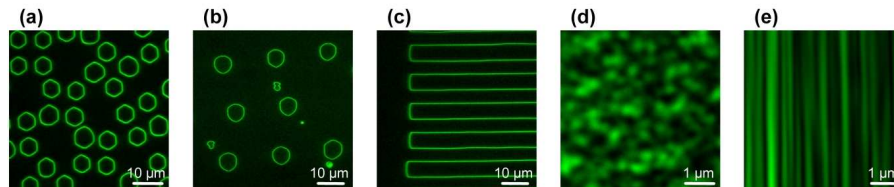


Fig. 3. Domain structures imaged by Čerenkov SHG, taken with the focal plane of the fundamental beam located $10 \mu\text{m}$ inside the corresponding NPS: (a) Congruent LiNbO_3 with 2D short-range ordered domain structure [31, 32, 33]. (b) Stoichiometric LiTaO_3 with 2D quasi-periodic domain structure [34]. (c) KTiOPO_4 with 1D periodic domain structure [35]. (d) and (e) As-grown $\text{Sr}_x\text{Ba}_{1-x}\text{Nb}_2\text{O}_6$ crystal with naturally random domain structure at X-Y and X-Z planes [36, 37], respectively.

The Čerenkov-type SHG laser scanning microscopy can also produce 3D images by stacking X-Y scans recorded at different depths inside the medium. Figure 4(a) shows such 3D image of the inverted domains distribution hidden inside the short-range ordered NPS [31, 32, 33],

from which one can determine the quality of poling in the bulk of the crystal. These images and subsequent movies were created using the ImageJ software. It is well known that the formation of a periodic domain structure having micron or submicron periods in ferroelectric materials is a very complicated process. There are large numbers of theoretical works that attempt to analyze and model this process, but most of them are still awaiting experimental verification. Here we show that Čerenkov-type SHG laser scanning microscopy may provide this necessary experimental evidences, because it enables direct visualization of the evolution of the domain structure beneath the surface. For example, by focusing the laser beam first on to the +Z surface of a NPS formed in congruent LiNbO₃ crystal and then imaging consecutively at different depths, we are able to show experimentally how the well-defined domains of initially (at the +Z surface) circular shape acquire hexagonal shape inside the crystal.

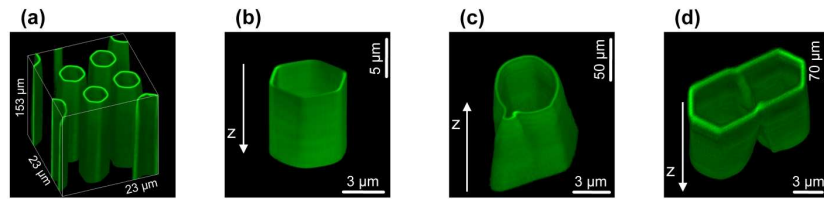


Fig. 4. Three dimensional visualization of inverted ferroelectric domains inside congruent LiNbO₃ crystal by Čerenkov-type second harmonic generation laser scanning microscopy. (a) Domain distribution in the nonlinear photonic structure. (b) Transformation from the initially circular to hexagonally shaped domains [(Media 1) 1(a) and (Media 2)1(b)]; (c) Formation of a defect during the domain growth [(Media 3)3(a) and (Media 4)2(b)]; (d) Merging of two initially separated ferroelectric domains[(Media 5) 3(a) and (Media 6)3(b)].

As shown in Fig. 4(b) [(Media 1) 1(a) and (Media 2)1(b)], the transition process occurs very near to the surface and terminates at a depth of about 1 μm below to the surface. This result provides an experimental support for the Roseman's model, in which the existence of a tangential electric field is regarded as the main reason for the sidewise growth of the inverted domains [17] and for the presence of hexagonal shapes [18]. In the model, it is predicted that the tangential electric field appears at the surface plane and decreasing to zero at a distance of half the period of defined domain structure, typically on the order of 10 μm . Hence, the transition of the shape of the reversed domains should occur very close to the surface, in good agreement with our experiment result. The Čerenkov-type SHG laser scanning microscopy allows also to study the process of defect formation in domain patterns. For example, Fig. 4(c) [(Media 3)Movie 2(a) and (Media 4)2(b)] shows the formation of reversed domain with irregular shape due to the very small defect in the domains pattern. In Fig. 4(d) [(Media 5) 3(a) and (Media 6)3(b)], we visualized the effect of merging of two initially separated neighboring domains. Note that the duty cycle of reversed domains in the bulk of the crystal may be significantly different from those measured at the surface. As shown in the graph and the movie, the two domains that are separated at the very surface gradually merge into a single domain inside the crystal. In some cases the domain merging process may be even more complicated and may present different features depending on the applied electric field, the distribution of defects inside the crystal, etc. In this particular case [Fig. 4(d)] the inverted upper right domain expands along the preferred diagonal direction of the hexagon, maintaining its hexagonal shape until it comes into contact with the other one. On the other hand, the expansion of the second domain starts simultaneously from two points, which seem to be just localized defects. As a result, this domain acquires almost a pentagon shape before it runs into the second domain. We believe that the existence of

such interesting spatial dynamics could not have been revealed without the effective imaging method.

4. Conclusion

We observed and characterized the Čerenkov type second harmonic generation at the boundaries between ferroelectric domains. We utilized this effect for direct 3D imaging of the antiparallel domains in nonlinear photonic structures in quadratic materials with sub-diffraction limit resolution. In particular, we visualized the geometry of the inverted domains in the bulk of the medium, showing details such as, e.g., transition of the domain shape from circular into hexagonal or merging of the individual domains into larger entity. The ability to extract such information will improve understanding of domain reversal process allowing better control of the fabrication of domain structures. Moreover, it provides characterization tools for expanding the modulation capabilities of nonlinear photonic crystals into the third dimension, along the crystal's Z axis. The Čerenkov-type SHG laser scanning microscopy is a very powerful tool that will further inspire the design and development of new and sophisticated nonlinear photonics structures for advanced photonic applications.

Acknowledgement

This work has been inspired by the late Solomon Saitiel. The authors acknowledge research support from the Max Planck Society, Chinese Academy of Science, Israel Science Foundation and Australian Research Council.